

PROCEEDINGS OF SPIE

[SPIDigitalLibrary.org/conference-proceedings-of-spie](https://spiedigitallibrary.org/conference-proceedings-of-spie)

New lithographic techniques for x-ray spectroscopy

Jake McCoy, Randall McEntaffer, Casey DeRoo

Jake McCoy, Randall McEntaffer, Casey DeRoo, "New lithographic techniques for x-ray spectroscopy," Proc. SPIE 9905, Space Telescopes and Instrumentation 2016: Ultraviolet to Gamma Ray, 990524 (27 July 2016); doi: 10.1117/12.2232072

SPIE.

Event: SPIE Astronomical Telescopes + Instrumentation, 2016, Edinburgh, United Kingdom

New lithographic techniques for X-ray spectroscopy

Jake McCoy^a, Randall McEntaffer^a, and Casey DeRoo^b

^aPennsylvania State University, University Park, PA, USA

^bHarvard-Smithsonian Center for Astrophysics, Cambridge, MA, USA

ABSTRACT

Off-plane reflection gratings require high-fidelity, custom groove profiles to perform with high spectral resolution in a Wolter-I optical system. This places a premium on exploring lithographic techniques in nanofabrication to produce state-of-the-art gratings. The fabrication recipe currently being pursued involves electron-beam lithography (EBL) and reactive ion etching (RIE) to define the groove profile, wet anisotropic etching in silicon to achieve blazed grooves and UV-nanoimprint lithography (UV-NIL) to replicate the final product. A process involving grayscale EBL and thermal reflow known as thermally activated selective topography equilibration (TASTE) is also being investigated as an alternative method to fabricate these gratings. However, a master grating fabricated entirely in soft polymeric resist through the TASTE process requires imprinting procedures other than UV-NIL to be explored. A commercially available process called substrate conformal imprint lithography (SCIL) has been identified as a possible solution to this problem. SCIL also has the ability to replicate etched silicon gratings with reduced trapped air defects as compared to UV-NIL, where it is difficult to achieve conformal contact over large areas. As a result, SCIL has the potential to replace UV-NIL in the current grating fabrication recipe.

Keywords: X-ray optics, diffraction gratings, off-plane gratings, spectroscopy, nanofabrication, electron-beam lithography, thermally activated selective topography equilibration, substrate conformal imprint lithography

1. INTRODUCTION

X-ray spectroscopy has been proven to be an extremely important aspect of high energy astrophysics. In addition to providing a powerful tool for performing diagnostics in astrophysical plasmas, high-resolution X-ray spectroscopy has direct applications to several key scientific issues including making measurements of the Warm-Hot Intergalactic Medium, determining elemental abundances in the local interstellar medium and studying dynamics in active galactic nuclei. The majority of astrophysically abundant X-ray spectral lines exist below 2 keV, at soft X-ray energies, necessitating the use of diffraction gratings to perform high-resolution spectroscopy. The grating spectrographs onboard *XMM-Newton* and the *Chandra X-ray Observatory* have resolving powers ($\lambda/\Delta\lambda$) on the order of several hundred and have provided large amounts of scientific return. Future X-ray observatories will require advanced spectrographs with $\lambda/\Delta\lambda$ of a few thousand to make significant improvements in X-ray spectroscopy and to address future scientific problems.

Due to the wavelength scale of soft X-rays, suitable reflection gratings must feature finely repeating groove structures that are periodic on the order of hundreds of nanometers or less. Though traditionally handled by mechanical ruling engines, fabricating gratings that push the state-of-the-art and will make significant advancement in the capabilities of future X-ray spectrographs requires utilizing techniques in the area of nanofabrication. This paper discusses the design of next-generation off-plane reflection gratings and outlines a fabrication recipe that consists of electron-beam lithography and multiple etching processes to create a master, carried out at the Pennsylvania State University Materials Research Institute, and an imprinting procedure for replication, provided by an external vendor. It also discusses the prospect of using techniques involving grayscale electron-beam lithography, selective thermal reflow and an alternative imprinting procedure to fabricate these gratings.

Further author information: (Send correspondence to J.M.)
J.M.: E-mail: jam1117@psu.edu

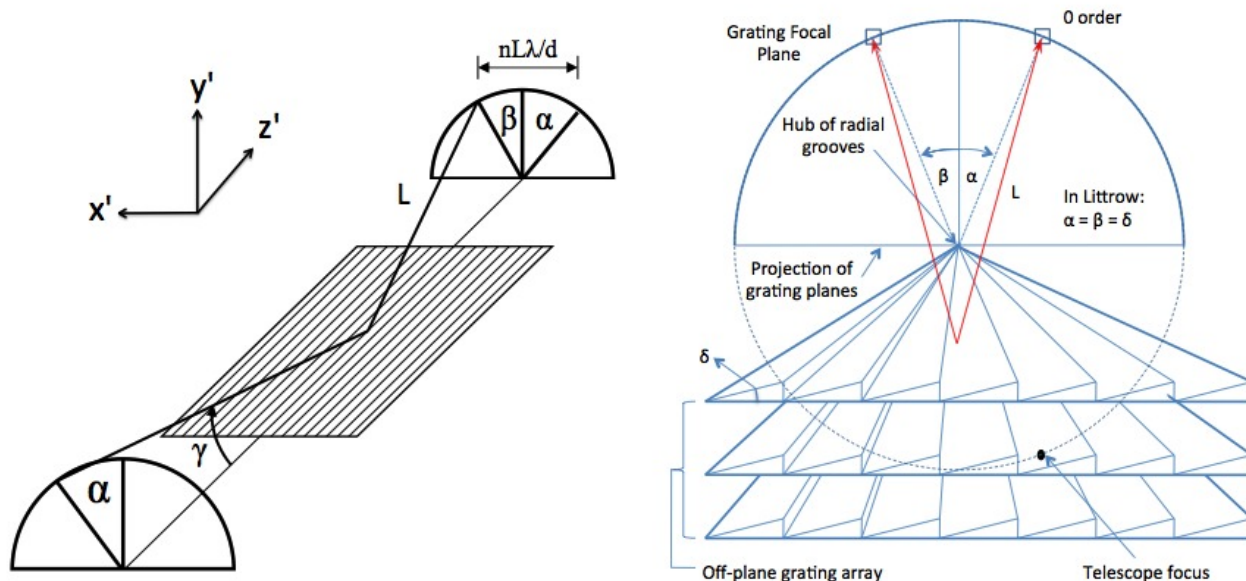


Figure 1. *Left:* The off-plane grating geometry.^{2,3} X-rays are incident at an angle α relative to the direction of the grooves at a grazing angle γ and diffracted to an angle β , forming a conical pattern. *Right:* Radially ruled, blazed off-plane gratings. Grooves are designed to match the converging beam of a telescope of some focal length and blazed to form a saw-tooth pattern with angle δ . Diffraction efficiency is maximized when $\alpha = \beta = \delta$.

2. OFF-PLANE GRATING SPECTROGRAPHS

The implementation of grazing incidence optics is key to realizing a modern X-ray telescope. For example, *XMM-Newton* and *Chandra* both employ a set of nested Wolter-I optics (a primary parabolic mirror, followed by secondary hyperbolic) with focal lengths of several meters. Planar reflection gratings can be integrated into such an optical system by being positioned to intercept the radiation coming to a focus. A detector, such as a CCD camera, placed at the focal plane can then be used to image the dispersed spectrum. Many spectrographs use classical, or ‘in-plane’, reflection gratings where the grooves are nearly perpendicular to the incoming radiation. However, gratings designed for conical, or ‘off-plane’, diffraction (Fig. 1) have several attractive features.¹ First, there is minimal groove shadowing at grazing incidence angles resulting in high diffraction efficiency. In addition, they feature lower scatter, have better spectral coverage than in-plane gratings, and have the potential for high resolving power. Further, off-plane gratings can be tightly packed into an array, offering an efficient way to be paired with Wolter-I optics in an X-ray telescope, to maximize collecting area for spectroscopy.

The location of diffracted orders for an off-plane grating is described by the generalized grating equation:

$$\sin(\alpha) + \sin(\beta) = \frac{n\lambda}{d \sin(\gamma)} \quad (1)$$

where α is the incidence angle, β is the diffracted angle and γ is the grazing angle, which defines the half angle of the cone aperture (see Fig. 1, left). Further, n is the diffracted order number, λ is the wavelength of the incident X-rays and d is the regular spacing between grooves so that $G = 1/d$ is the groove density. In an off-plane grating spectrograph, the grating grooves are oriented quasi-parallel to the optical axis of the telescope, termed the z' direction. X-rays incident on the grating at a given z' coordinate along the grating will travel a distance L to the focal plane. Although diffracted orders lie on the surface of a cone, λ -dependent dispersion can be shown to occur only in the x' direction (in the plane of the grating, but perpendicular to the direction of the grooves). Then, linear dispersion in x' at the focal plane for a given n is proportional to L and G . In a space-borne off-plane grating spectrograph, the focal length, and hence L , may be limited to several meters. As a result, groove densities G of 5,000 grooves/mm or more ($d = 200$ nm or less) are required to achieve high spectral resolution ($\lambda/\Delta\lambda$ of a few thousand) in such a spectrograph system.

In principle, gratings with parallel grooves lead to aberrations when dispersing a spectrum from a converging beam of radiation.⁴ This can be remedied by designing off-plane gratings that have a radially ruled groove profile such that G linearly increases in the z' direction, along the length of the grating (Fig. 1, right). From the above discussion $L = L(z')$ while G stays constant for a parallel ruled grating; this leads to varying linear dispersion at the focal plane. With a radially ruled grating, the $G = G(z')$ dependence compensates for the $L(z')$ variation that arises from a broad, converging beam incident on the grating. Additionally, the radially ruled grooves match the convergence of the telescope such that α stays constant over the length of the grating, eliminating further aberrations. In practice however, such a radial profile is usually approximated with an off-plane variable line space (VLS) profile consisting of several sections of parallel grooves with increasing G toward the focal plane. The fidelity of this approximation is limited by minimum tool step size (typically at the sub-nm level), which directly translates to Δd between each section of grooves.

Achieving high throughput (system effective area of several hundred cm^2) in an off-plane grating spectrograph requires hundreds, or even thousands of gratings to be stacked and aligned in modular arrays.⁵ Each grating thus should be relatively large in area (several tens of cm^2) and perform with excellent diffraction efficiency. Gratings with groove facets blazed to a triangular saw-tooth profile (Fig. 1, right) will preferentially disperse X-rays to one side of zero order, effectively doubling signal-to-noise in the detected spectrum with half the number of necessary detector elements. Additionally, the blaze angle δ can be chosen to maximize efficiency at a certain bandpass when in Littrow configuration: $\alpha = \beta = \delta$. This bandpass is centered on the blaze wavelength given by

$$\lambda_b = \frac{2d \sin(\gamma) \sin(\delta)}{n} \quad (2)$$

To prevent scatter from degrading performance of the grating, facet surfaces must be smooth to 1 nm RMS or less. Further, any bow in the figure of these gratings will induce a local change in pitch or roll, which must be kept within alignment tolerances. The figure of each grating should thus be as flat as possible, which is largely dependent on the type of substrate employed. All of this considered, the performance of an off-plane grating spectrograph depends heavily on how the gratings are fabricated in the cleanroom. The general course of action is to fabricate a master grating template featuring radially ruled, blazed grooves with high density and implement a procedure for producing replicas that will be stacked and aligned into modular arrays.

3. GRATING FABRICATION

Fabrication procedures for X-ray diffraction gratings have evolved significantly in recent years. Gratings with a sinusoidal groove profile can be fabricated using holographic lithography.⁶ Due to the simultaneous nature of this patterning method, large area gratings are readily producible. However, because a curved groove pattern is produced when the recording lasers are offset, it is not possible to produce a radial profile with this technique. Parallel ruled gratings fabricated through this technique have been flown in aligned modules on several sub-orbital rockets.⁷⁻¹⁰ These gratings can be blazed to an approximate triangular profile with ion-etching.¹¹ However, these types of gratings have been found to exhibit significant amounts of scatter.¹² Further, groove density is limited by the wavelength of the recording lasers used. These limitations led to the development of a recipe based in anisotropic etching and the investigation of techniques involving grayscale electron-beam lithography.

3.1 Anisotropic etching

Anisotropic etching processes in monocrystalline silicon (Si) have previously been used to fabricate blazed reflection gratings for X-ray telescope applications.^{2,3,13-15} Multilayer coated blazed gratings for monochromator applications have also recently been fabricated in a similar manner.¹⁶ The central step in manufacturing these type of gratings is performing an anisotropic wet etch in Si with potassium hydroxide (KOH) over long, narrow, rectangular areas which define the placement of grooves for the final product. KOH etching in Si is based on the principle that etch rates in the crystal for $\langle 100 \rangle$ directions are much higher than $\langle 111 \rangle$ directions, where $\langle hkl \rangle$ are Miller indices. The result of such an etch is a collection of long, atomically smooth troughs defined by exposed $\{111\}$ planes. These troughs, which provide the blazed profile for the grating, appear as a triangular saw-tooth when viewed side-on. The angular orientation δ of these groove facets is set by choosing an appropriate off-axis cut Si wafer for etching.^{3,17,18} To define the placement of these grooves, a pattern must be created in a thin film

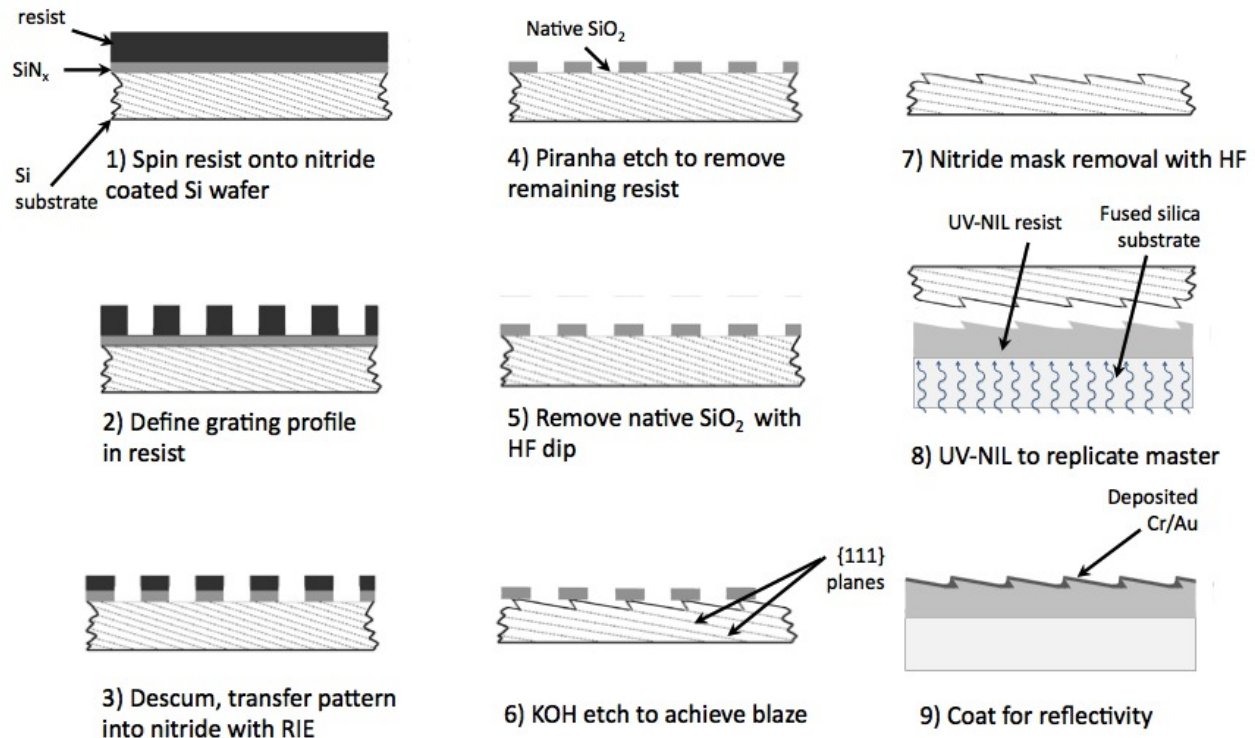


Figure 2. Outline of fabrication recipe for gratings based on KOH etching in crystalline Si to produce blazed groove facets.^{2,3,13-15} A laminar grating pattern (i.e. a square wave), defining the off-plane VLS groove profile, is patterned into EBL resist. This pattern is transferred into the thin SiN_x film below via RIE. The underlying Si wafer is KOH etched through this groove pattern to create blazed groove facets defined by $\langle 111 \rangle$ crystallographic orientations. The etched Si master is replicated with an imprinting process provided by Nanonex Corporation, and each is coated for soft X-ray reflectivity.

of material which is insoluble in KOH, such as a silicon nitride (SiN_x). One approach in producing this pattern is to perform a reactive ion etch¹⁸ (RIE) in a fluorocarbon (CHF₃) and oxygen (O₂) mixture to achieve a controlled anisotropic etch through the SiN_x film. However, due to the global nature this dry etching process, the desired pattern must first be defined in a layer of polymeric resist on top of the film. There are a variety of lithographies apt to produce such a pattern in resist, including interference lithography¹⁹ (IL), nanoimprint lithography²⁰ (NIL) and electron-beam lithography²¹ (EBL). IL has been used to accurately pattern parallel grooves for this purpose¹³⁻¹⁵ but it is not straightforward to produce a VLS profile through this technique. Thermal NIL (T-NIL) has been used to pattern a custom off-plane VLS profile in resist with a pre-master fabricated by LightSmyth Technologies^{2,3*}. However, in addition to it being a challenge to align the pre-master with the crystallographic planes of Si, defects from the imprinting process have been observed. Though time-consuming and hence expensive for large areas, EBL is a well-established technique for directly writing custom patterns into resist, such as a VLS groove profile.¹⁶ Additionally, there is potential for implementing a procedure to align EBL design coordinates with exposed crystallographic plane intersections.

The fabrication recipe currently being pursued, outlined in Fig. 2, first uses EBL to pattern laminar grooves in a ~100 nm thick layer of ZEP520A resist, spun onto a 6" Si wafer that is coated with ~30 nm of SiN_x. An off-plane VLS profile, approximating radially ruled grooves, is written over a 96 mm by 75 mm area (72 cm²). A Vistec EBLPG 5200 EBL tool is used to write several sections of parallel grooves with groove spacings ranging from $d = 160$ nm to $d = 158.25$ nm, in steps of $\Delta d = 0.25$ nm. An O₂ RIE descum process is then performed to remove residual resist in these troughs. This way, a clean etch through the SiN_x film is achieved upon performing a RIE with CHF₃ and O₂, which exposes the surface of the Si wafer. A piranha etch (mixture of sulfuric acid

*<http://www.lightsmyth.com/>

and hydrogen peroxide) is carried out to remove the remaining resist, leaving just the patterned SiN_x film on the Si wafer. After native silicon dioxide (SiO_2) is removed with a hydrogen fluoride (HF) dip, a timed KOH etch is performed to achieve the blazed saw-tooth pattern for the grating. Removing the SiN_x with HF leaves an etched Si master grating template suitable for replication. Currently, this master template is replicated via UV-NIL²² through Nanonex Corporation[†] in a proprietary UV-curable resist on a UV-transparent fused silica substrate. A benefit of imprinting on a fused silica substrate is that, in contrast to standard Si wafers, they are often flat enough for off-plane grating alignment tolerances⁵ (typically $<2 \mu\text{m}$ peak-to-valley for 6" wafers). Finally, each replica is coated with a chromium/gold layer for reflectivity at soft X-ray wavelengths and the process is complete.

3.2 Grayscale electron-beam lithography

Grayscale EBL (GEBL) is a technique used to directly pattern nm-sized 3D structures in polymeric resist. In contrast to standard EBL which involves just two doses $D_0 = 0$ (unexposed) and D_{clear} (dose-to-clear) to pattern bi-level structures, GEBL uses a range of doses $D_0 < D < D_{\text{clear}}$ to achieve resist thicknesses between the deposited spin coat layer and the surface of the substrate to produce a 3D structure such as a staircase²³ (see Fig 3, left). Then, such a stepped structure can be smoothed into a wedge-like structure through the process of thermally activated selective topography equilibration²⁴ (TASTE). Based on polymer thermal reflow,^{25–27} TASTE hinges on the principle that for a positive tone resist, electron dose D locally reduces the average molecular weight M_w of the polymer chains throughout the depth of the resist and hence the glass-liquid transition temperature T_g of the material (see Fig 3, right). When heated above T_g , the resist is able to flow with a M_w -dependent viscosity. Consider a staircase structure consisting of an unexposed region with spin coat thickness h_0 , N electron-exposed steps with thicknesses h_i (where i is an integer between 1 and N), and a region that has been cleared to the substrate with $h = 0$ (see Fig. 3 for $N = 3$). GEBL exposure causes M_w of the unexposed resist, $M_{w,0}$, to be significantly higher than any of the exposed steps with $M_{w,i}$. As a result, T_g of the unexposed resist, $T_{g,0}$, also will be higher than any of the exposed steps with $T_{g,i}$. For poly(methyl methacrylate) (PMMA)^{24–27} and ZEP520A²⁸ resist systems, there exist process windows for the entire sample to be globally heated to a temperature $T_{g,0} > T_{\text{reflow}} > T_{g,1}$ so that the exposed steps with thicknesses h_i will flow into a smooth surface while the unexposed steps with thicknesses h_0 remain largely unaffected. By patterning such staircase structures regularly spaced at a pitch d over a large area, and thermally treating the entire sample (see Fig. 4, left), TASTE has the potential for the fabrication of a master grating template.

In TASTE, the exposed resist is heated to a temperature $T_{g,0} > T_{\text{reflow}} > T_{g,1}$ where it is able to flow according to a visco-elastic behavior.^{28,30} As gravity can be neglected on the small size scales considered, evolution of the molten polymer, pinned between the unexposed step and the substrate, is dominated by surface tension forces.^{25,30,31} During this reflow process, wetting forces at the polymer-substrate interface drive the molten polymer to creep along the substrate. At this interface, there is an apparent contact angle that evolves during the reflow process.^{28,30} The optimization of this contact angle should be of interest when fabricating a groove facet with blaze angle δ via TASTE. In addition to flatness considerations discussed in section 2, the choice of substrate used for the process therefore becomes important when considering the wetting forces involved. Further, the speed of the reflow process depends on the viscosity of the molten polymer, which in turn depends on M_w and T_{reflow} . All of this considered, producing smooth, linear groove facets via TASTE is an optimization problem involving many parameters which requires extensive experimentation to implement process development. Simulations can also be carried out to model the reflow process with open-source software packages such as Surface Evolver^{30†}.

Optimizing the TASTE process for producing saw-tooth gratings with a smooth blaze first requires fabricating the appropriate structure in resist with GEBL. Because D needs to be carefully controlled to produce 3D patterns with high precision, a low contrast resist-developer system should be implemented and the proximity effect³² must be corrected for, which can be handled with algorithms contained in the GenISys BEAMERTM software package[‡]. Careful field stitching during GEBL exposure is also of high importance to prevent irregularities in the

[†]<http://www.nanonex.com/>

[‡]<http://facstaff.susqu.edu/brakke/evolver/evolver.html>

[§]<http://genisysgmbh.de/web/products/beamer.html>

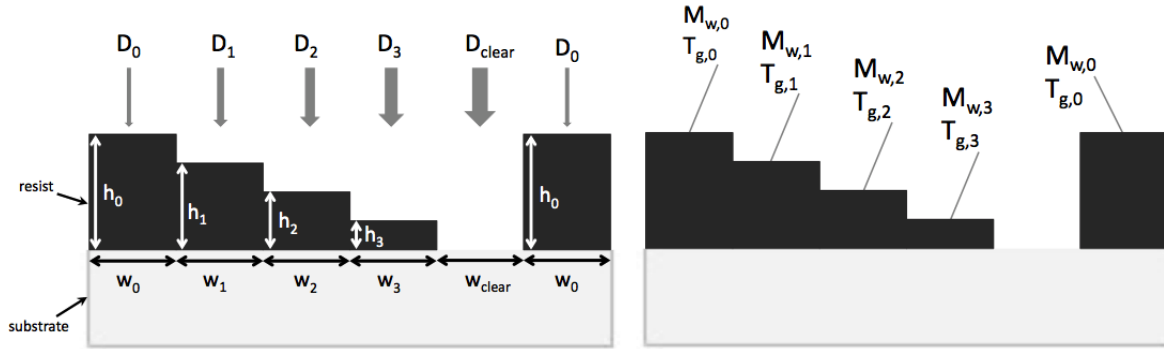


Figure 3. Some basic properties of a positive tone polymeric resist (i.e. PMMA or ZEP520A) arising from a GEBL process to create a stepped structure.^{24–28} *Left:* Dose-modulated electron beam exposure results in varying resist thicknesses after wet development. An electron dose $D_0 = 0$ retains the original spin coat thickness h_0 while D_{clear} clears the resist down to the substrate. Electron doses $D_0 < D_1 < D_2 < D_3 < D_{\text{clear}}$ result in resist thicknesses $h_0 > h_1 > h_2 > h_3 > 0$. Lateral widths w_0, w_1, w_2, w_3 and w_{clear} depend on the design of the GEBL pattern. *Right:* Varying resist thicknesses result from the M_w -dependent etch rates involved in wet development. Electron doses $D_0 < D_1 < D_2 < D_3 < D_{\text{clear}}$ result in average polymer molecular weights $M_{w,0} > M_{w,1} > M_{w,2} > M_{w,3} > M_{w,\text{clear}}$, where resist with $M_{w,\text{clear}}$ gets completely etched away during wet development. The glass-liquid transition temperature T_g of polymers also depends on M_w . Steps in the developed structure with $M_{w,0} > M_{w,1} > M_{w,2} > M_{w,3}$ locally have $T_{g,0} > T_{g,1} > T_{g,2} > T_{g,3}$. When the entire structure is heated globally to a temperature $T_{g,0} > T_{\text{reflow}} > T_{g,1}$ via TASTE,²⁴ the exposed steps are able to flow into a smooth surface. Meanwhile, the unexposed portion with thickness h_0 remains relatively unaffected, providing an approximately vertical sidewall. In this way the TASTE process has the potential to create blazed groove facets suitable for a grating.

grating. Further, lateral step widths w_i should be chosen in relation to the spin coat thickness h_0 to get a quality outcome from the wet development process. In EBL, it is difficult to write patterns with high aspect ratios; for simplicity, it is beneficial design the structure so that $w_i \approx h_0$. Following this rule of thumb, a groove facet with a blaze angle $\delta \approx 45^\circ$ in principle could be realized starting from a GEBL design with just one intermediate step in the staircase ($N = 1$) with a lateral width $w_1 = h_0$ and some thickness $h_1 \approx h_0/2$ (see Fig. 4, left). The blaze angle δ could then be reduced by widening this step, or by adding more steps to the staircase. The reflow process must be optimized to produce a structure with a smooth, linear slope from the intermediate step with thickness h_1 . Further, although $T_{\text{reflow}} < T_{g,0}$, the unexposed step still will be affected by the reflow process in the sense that sharp corners will be rounded and the initially vertical sidewall angle will be shallowed slightly. The pitch of such a grating that utilizes one intermediate GEBL step is nominally $d = w_0 + w_1 + w_{\text{clear}}$. Achieving fine pitch would then require starting with a thin spin coat thickness h_0 to achieve a sufficiently small w_1 . Lateral widths w_0 and w_{clear} should be kept small to minimize specular reflection in the final product.

The TASTE process has the potential to fabricate off-plane gratings with flexible groove shape and custom groove profiles. However, due to the cost and difficulty of the procedure, TASTE is best suited to create a master grating template for replication. However, in contrast to etched Si, structures created in resist are often too soft to stand up against UV-NIL processes. One exception is hydrogen silsesquioxane (HSQ), which has been demonstrated to be hard enough for direct stamping using T-NIL.³³ However, thermal reflow has not been proven successful with this resist system. These limitations led to the investigation of an alternative, commercially available[¶] imprinting procedure called substrate conformal imprint lithography (SCIL).²⁹ In contrast to T-NIL and UV-NIL, which use hard stamps, the SCIL process hinges on forming a composite stamp from the master grating template that is used for imprinting (see Fig. 4, right). This allows the master grating to be made from a soft material, such as PMMA or ZEP520A. The composite stamp is molded in a thin layer of a polydimethylsiloxane (PDMS)-based material with an increased Young's modulus compared to PDMS materials used in standard soft lithography,³⁴ which allows for the replication of nm-sized structures. This mold is glued with soft PDMS to a thin glass plate, which is flexible in the out-of-plane direction but rigid in the in-plane direction. Because this composite stamp is flexible, it is able to conform to whatever slight bow the replica

[¶]SCIL solutions are available commercially from Philips SCIL Nanoimprint Solutions (<http://www.ip.philips.com>) and SUSS Mircotec (<http://www.suss.com/>).

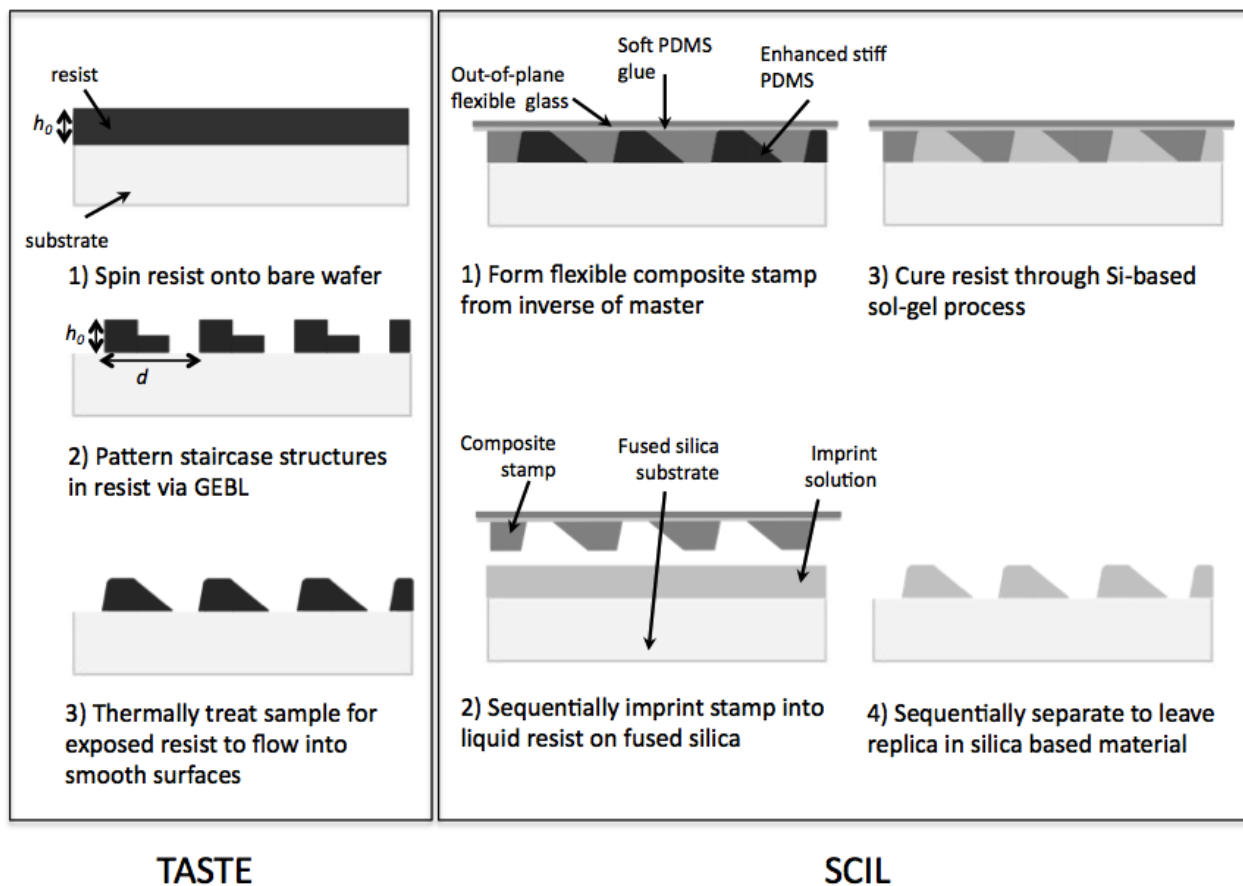


Figure 4. Outline of proposed recipe to fabricate gratings using TASTE²⁴ to create a master template in polymeric resist (PMMA or ZEP520A) and SCIL²⁹ to produce replicas in silica. *Left:* The TASTE process has the potential to produce blazed groove facets starting from a GEBL staircase structure with just one intermediate step. The selective thermal reflow process can be optimized to achieve a linear slope from the exposed step being heated above its T_g . However, unexposed regions inevitably will be affected: sharp corners will be rounded and the initially vertical sidewall resulting from GEBL will be shallowed slightly. *Right:* Features created in soft resist can be replicated via SCIL. A flexible composite stamp is formed from the master template with features that are rigid enough to replicate nm-sized structures. The stamp is sequentially imprinted into liquid resist with a specialized pneumatic tool to achieve conformal contact with the replica substrate. The resist forms a gel through a chemical sol-gel process and gradually dries into solid silica. Then, the stamp is sequentially separated to leave the replicated structure in silica.

substrate may have. This results in a significant reduction of trapped air pockets and damage due to particulate contaminants compared to what arises when practicing T-NIL or UV-NIL over large areas (several tens of cm²). To achieve conformal contact, the SCIL imprinting process uses a specialized pneumatic tool to sequentially imprint the stamp into a liquid resist^{||}. This imprint resist forms stable replicated features in silica through a Si-based sol-gel process.³⁵ During this imprinting procedure, chemical reaction products and small pockets of trapped are able to diffuse into the composite stamp. In summary, SCIL is a commercially available replication procedure compatible with nm-sized soft polymeric features and is a viable alternative to standard nanoimprint lithographies, beneficial especially for replicating gratings over large areas.

4. CONCLUSION

Off-plane gratings for astronomical soft X-ray spectrographs are currently being fabricated at the Pennsylvania State University Materials Research Institute through EBL, anisotropic etching and UV-NIL, as discussed in section 3.1. These common nanofabrication procedures are successful in producing large-format, approximately radially ruled gratings with high groove density and smoothly blazed groove facets. Results on diffraction efficiency and spectral resolving power will be presented in forthcoming papers.

TASTE is an alternative approach to fabricate a master grating template entirely in resist. Though exploratory, this techniques offers several benefits. TASTE has the potential to fabricate a master template in essentially two steps, eliminating the need for multiple etching processes: GEBL to create a repeating staircase structure in resist and a global thermal treatment (i.e. via hotplate) to achieve smooth surfaces for a blaze. In contrast to KOH etching in Si, TASTE is flexible in producing grooves with different shapes and blaze angles. Further, because it does not involve any substrate etching, there is no need for crystallographic plane alignment; a TASTE grating potentially could be fabricated directly on a flat fused silica substrate. However, this approach also comes with difficulties and challenges to overcome. In particular, achieving sub-nm RMS surface roughness for the blazed facets will require optimal reflow conditions and careful analysis of the temperature-dependent polymer viscosities and wetting forces involved. Additionally, excellent field stitching and long write times are needed to produce a large-format grating pattern through GEBL.

SCIL provides a way to produce grating replicas from a master template made in resist that is too soft to stand up against UV-NIL. However, it also offers benefits applicable to the replication of large-format gratings in general. As discussed in section 3.2, the flexible nature of the composite stamp used in SCIL allows for conformal contact to be made with the replica substrate. This is particularly difficult to achieve with UV-NIL over large areas (several tens of cm²), which results in defects that arise from trapped air pockets present during the imprinting process. Imprinting with a composite stamp also reduces damage from particulate contamination and allows small trapped air pockets to diffuse into the stamp. SCIL thus may be more apt than UV-NIL to replicate a large-format etched Si master. The implementation of SCIL into the anisotropic etching recipe is currently being pursued in collaboration with the University of Pennsylvania Singh Center for Nanotechnology and Philips SCIL Nanoimprint Solutions.

ACKNOWLEDGMENTS

Special thanks are due to Dr. Gerald Lopez and Dr. Roger McCay at GenISys GmbH, Dr. Vitaliy Guzenko and Dr. Robert Kirchner at the Paul Scherrer Institut, Dr. Marc Verschuuren at Philips SCIL Nanoimprint Solutions and Dr. Dmitriy Voronov Lawrence Berkeley National Laboratory. This work was supported by a NASA Space Technology Research Fellowship.

REFERENCES

- [1] Cash, Jr., W. C., "X-ray optics. II - A technique for high resolution spectroscopy," *Appl. Opt.* **30**, 1749–1759 (1991).

^{||}For a demonstration, see the video embedded at suss.com/scil

- [2] McEntaffer, R., DeRoo, C., Schultz, T., Gantner, B., Tutt, J., Holland, A., O'Dell, S., Gaskin, J., Kolodziejczak, J., Zhang, W. W., Chan, K.-W., Biskach, M., McClelland, R., Iazikov, D., Wang, X., and Koecher, L., "First results from a next-generation off-plane X-ray diffraction grating," *Experimental Astronomy* **36**, 389–405 (2013).
- [3] DeRoo, C. T., McEntaffer, R. L., Miles, D. M., Peterson, T. J., Marlowe, H., Tutt, J. H., Donovan, B. D., Menz, B., Burwitz, V., Hartner, G., Allured, R., Smith, R. K., Gnther, R., Yanson, A., Vacanti, G., and Ackermann, M., "Line spread functions of blazed off-plane gratings operated in the littrow mounting," *Journal of Astronomical Telescopes, Instruments, and Systems* **2**(2), 025001 (2016).
- [4] Cash, Jr., W. C., "X-ray spectrographs using radial groove gratings," *Appl. Opt.* **22**, 3971–3976 (1983).
- [5] Allured, R. and McEntaffer, R. T., "Analytical alignment tolerances for off-plane reflection grating spectroscopy," *Experimental Astronomy* **36**, 661–677 (2013).
- [6] Burrow, G. M. and Gaylord, T. K., "Multi-beam interference advances and applications: nano-electronics, photonic crystals, metamaterials, subwavelength structures, optical trapping, and biomedical structures," *Micromachines* **2**(2), 221–257 (2011).
- [7] McEntaffer, R. L. and Cash, W., "Soft X-Ray Spectroscopy of the Cygnus Loop Supernova Remnant," *ApJ* **680**, 328–335 (2008).
- [8] Oakley, P., Cash, W., McEntaffer, R., Shipley, A., and Schultz, T., "The EXOS sounding rocket payload," *Proc. SPIE* **7437**, 74370I (2009).
- [9] Zeiger, B., Shipley, A., Cash, W., Rogers, T., Schultz, T., McEntaffer, R., and Kaiser, M., "The CODEX sounding rocket payload," *Proc. SPIE* **8076**, 80760S (2011).
- [10] Rogers, T., Schultz, T., McCoy, J., Miles, D., Tutt, J., and McEntaffer, R., "First results from the OGRESS sounding rocket payload," *Proc. SPIE* **9601**, 960104 (2015).
- [11] Aoyagi, Y. and Namba, S., "Blazed ion-etched holographic gratings," *Optica Acta: International Journal of Optics* **23**(9), 701–707 (1976).
- [12] McEntaffer, R. L., Osterman, S. N., Cash, W. C., Gilchrist, J., Flamand, J., Touzet, B., Bonnemason, F., and Brach, C., "X-ray performance of gratings in the extreme off-plane mount," *Proc. SPIE* **5168**, 492–498 (2004).
- [13] Franke, A. E., Schattenburg, M. L., Gullikson, E. M., Cottam, J., Kahn, S. M., and Rasmussen, A., "Super-smooth x-ray reflection grating fabrication," *Journal of Vacuum Science Technology B: Microelectronics and Nanometer Structures* **15**, 2940–2945 (1997).
- [14] Chang, C.-H., "Fabrication of sawtooth diffraction gratings using nanoimprint lithography," *Journal of Vacuum Science Technology B: Microelectronics and Nanometer Structures* **21**, 2755 (2003).
- [15] Chang, C.-H., "High fidelity blazed grating replication using nanoimprint lithography," *Journal of Vacuum Science Technology B: Microelectronics and Nanometer Structures* **22**, 3260 (2004).
- [16] Voronov, D. L., Anderson, E. H., Cambie, R., Cabrini, S., Dhuey, S. D., Goray, L. I., Gullikson, E. M., Salmassi, F., Warwick, T., Yashchuk, V. V., and Padmore, H. A., "A 10,000 groove/mm multilayer coated grating for EUV spectroscopy," *Optics Express* **19**, 6320 (2011).
- [17] Franssila, S., [*Introduction to Microfabrication, Chapter 4: Silicon*], 35–46, John Wiley & Sons, Ltd (2010).
- [18] Franssila, S., [*Introduction to Microfabrication, Chapter 11: Etching*], 127–141, John Wiley & Sons, Ltd (2010).
- [19] Lu, C. and Lipson, R., "Interference lithography: a powerful tool for fabricating periodic structures," *Laser & Photonics Reviews* **4**(4), 568–580 (2010).
- [20] Chou, S. Y., Krauss, P. R., and Renstrom, P. J., "Nanoimprint lithography," *Journal of Vacuum Science Technology B: Microelectronics and Nanometer Structures* **14**, 4129–4133 (1996).
- [21] Chen, Y., "Nanofabrication by electron beam lithography and its applications: A review," *Microelectronic Engineering* **135**, 57–72 (2015).
- [22] Haisma, J., Verheijen, M., van den Heuvel, K., and van den Berg, J., "Mold-assisted nanolithography: A process for reliable pattern replication," *Journal of Vacuum Science Technology B: Microelectronics and Nanometer Structures* **14**, 4124–4128 (1996).

- [23] Stauffer, J. M., Oppliger, Y., Regnault, P., Baraldi, L., and Gale, M. T., "Electron beam writing of continuous resist profiles for optical applications," *Journal of Vacuum Science Technology B: Microelectronics and Nanometer Structures* **10**, 2526–2529 (1992).
- [24] Schleunitz, A., Guzenko, V. A., Messerschmidt, M., Atasoy, H., Kirchner, R., and Schiff, H., "Novel 3D micro- and nanofabrication method using thermally activated selective topography equilibration (TASTE) of polymers," *Nano Convergence* **1**, 7 (2014).
- [25] Schleunitz, A. and Schiff, H., "Fabrication of 3D nanoimprint stamps with continuous reliefs using dose-modulated electron beam lithography and thermal reflow," *Journal of Micromechanics and Microengineering* **20**(9), 095002 (2010).
- [26] Schleunitz, A., Guzenko, V. A., Schander, A., Vogler, M., and Schiff, H., "Selective profile transformation of electron-beam exposed multilevel resist structures based on a molecular weight dependent thermal reflow," *Journal of Vacuum Science Technology B: Microelectronics and Nanometer Structures* **29**(6), 06F302 (2011).
- [27] Schleunitz, A., Spreu, C., Vogler, M., Atasoy, H., and Schiff, H., "Combining nanoimprint lithography and a molecular weight selective thermal reflow for the generation of mixed 3D structures," *Journal of Vacuum Science Technology B: Microelectronics and Nanometer Structures* **29**(6), 06FC01 (2011).
- [28] Kirchner, R., Guzenko, V., Vartiainen, I., Chidambaram, N., and Schiff, H., "Zep520a a resist for electron-beam grayscale lithography and thermal reflow," *Microelectronic Engineering* **153**, 71 – 76 (2016).
- [29] Verschuuren, M. A., *Substrate conformal imprint lithography for nanophotonics*, PhD thesis, Utrecht University (2010).
- [30] Kirchner, R., Schleunitz, A., and Schiff, H., "Energy-based thermal reflow simulation for 3D polymer shape prediction using Surface Evolver," *Journal of Micromechanics and Microengineering* **24**(5), 055010 (2014).
- [31] Chen, Y., Yi, A. Y., Yao, D., Klocke, F., and Pongs, G., "A reflow process for glass microlens array fabrication by use of precision compression molding," *Journal of Micromechanics and Microengineering* **18**(5), 055022 (2008).
- [32] Pavkovich, J. M., "Proximity effect correction calculations by the integral equation approximate solution method," *Journal of Vacuum Science Technology B: Microelectronics and Nanometer Structures* **4**, 159–163 (1986).
- [33] Gadegaard, N. and McCloy, D., "Direct stamp fabrication for {NIL} and hot embossing using {HSQ}," *Microelectronic Engineering* **84**(12), 2785 – 2789 (2007).
- [34] Xia, Y. and Whitesides, G. M., "Soft Lithography," *Annual Review of Materials Science* **28**, 153–184 (1998).
- [35] Hench, L. L. and West, J. K., "The sol-gel process," *Chemical Reviews* **90**(1), 33–72 (1990).